Microscopic realizations of the trap model

2004 J. Phys. A: Math. Gen. 37 3945

(http://iopscience.iop.org/0305-4470/37/13/003)

INSTITUTE OF PHYSICS PUBLISHING JOURNAL OF PHYSICS A: MATHEMATICAL AND GENERAL

J. Phys. A: Math. Gen. **37** (2004) 3945–3965 PII: S0305-4470(04)73885-8

Microscopic realizations of the trap model

I Junier and J Kurchan

PMMH UMR 7636 CNRS-ESPCI, Ecole Supérieure de Physique et Chimie Industrielles, 10, rue Vauquelin, 75231 Paris Cedex 05, France

Received 22 December 2003
Published 17 March 2004
Online at stacks.iop.org/JPhysA/37/3945 (DOI: 10.1088/0305-4470/37/13/003)

Abstract

Monte Carlo optimizations of number partitioning and of Diophantine approximations are microscopic realizations of 'trap model' dynamics. This offers a fresh look at the physics behind this model, and points at other situations in which it may apply. Our results strongly suggest that in any such realization of the trap model, the response and correlation functions of smooth observables obey the fluctuation–dissipation theorem even in the aging regime. Our discussion of the number partitioning problem may be relevant for the class of optimization problems whose cost function does not scale linearly with the size, and are thus awkward from the statistical mechanic point of view.

PACS numbers: 75.10.Nr, 05.20.−y, 64.70.Pf

(Some figures in this article are in colour only in the electronic version)

1. Introduction

During the last half century different models have been proposed to capture the dynamical properties of glasses. Among the phenomenological approaches, an illuminating and extensively studied minimal one is the 'trap model' proposed by Bouchaud [1]. It is based on the following picture: a particle evolves in a landscape energy that resembles a golf course with holes whose depths h are exponentially distributed following $\sim e^{-\beta_c h}$.

At each microscopical time, the particle emerges from a hole to a *horizon level* with a probability $\sim e^{-\beta h}$. Once escaped, it immediately falls in a new hole, which is in many applications randomly chosen (i.e. figure 1 is infinite dimensional). By construction, once the particle escapes from a hole, it totally loses memory and the system can be considered as reinitialized. The combination of exponential distribution of depths with an exponential probability of emerging, yields trapping times following a distribution whose mean diverges if $\beta > \beta_c$. Glassy behaviour results from the possibility of falling in holes with arbitrary long trapping times. We have the apparent paradox that if we consider any two times such that the system has just emerged from a trap, the dynamics is (statistically) reversible in

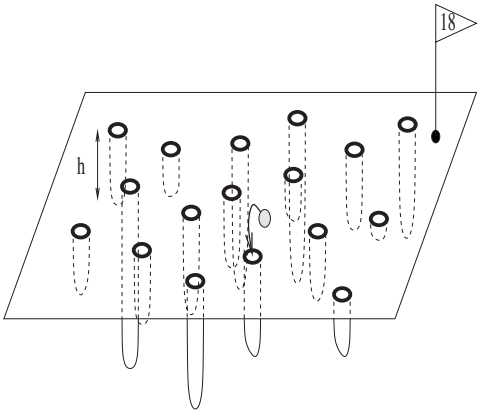

Figure 1. Schematic view of the phase space.

time: irreversibility arises only because at the end of a fixed interval the system is most probably in a long-lived trap.

These elements, existence of a horizon level up to which the system has to reemerge each time[1], time reversibility and the exponential density of states can be taken as the defining features of the model. Even if such particle behaviour has not been observed, this phenomenological approach gives many glassy features we can find in both structural and spin glasses. On the other hand, only recently trap model dynamics was shown to result for a microscopic model (the random energy model) endowed with a microscopic stochastic dynamics [2][2]—somewhat surprisingly given that the original motivation for the model was the phase-space structure of mean-field glass models.

Having microscopic realizations of the trap model is interesting, because it highlights physical situations when it may be relevant. There is a further reason: when it comes to studying the response of the dynamics to perturbations, the trap model allows a wide range of possibilities [3–5]: the reason for this is that, although it is quite clear how traps are affected by a perturbation, there is no unique prescription for how a perturbing field should affect the 'horizon', and through it the transition probabilities. This is an important issue, since response functions (especially the fluctuation–dissipation relation) have turned out to be amongst the most eloquent observables of glasses [6].

In this paper we study two examples yielding trap model dynamics: the number partitioning problem (NPP)—itself a form of packing problem, and Diophantine approximations. The NPP can be stated as follows: given N random numbers drawn from a uniform distribution [0, 1], divide them into two sets such that their sums are as close as possible. This is a caricature packing problem because if we consider N coins with independent random thicknesses, this corresponds to finding the minimal box height where they will fit in two piles. The Diophantine approximations we shall consider are of the following kind: find integer numbers n and m such that $n\sqrt{2} + m\sqrt{3}$ is as close as possible to a rational number.

The paper is organized as follows. In section 2 we study the NPP from the dynamical point of view. In section 3 we briefly describe how the problem of improving Diophantine approximations yields the same kind of dynamics. In the final section, we use these results to

[1] The reader familiar with mean-field glass models will wonder if this coincides with the 'threshold' level arising there. In fact, it does not: dynamics just below the threshold does not involve either reinitialization or reemerging, except possibly at very late times.

[2] To make the proof tractable, the dynamics chosen already assumes an escape time exponential in the depth, although we believe this is not essential.

discuss which features seem necessary for a model to have trap model-like dynamics, and we point out that when this happens, the fluctuation–dissipation theorem is obeyed, at least for smooth observables.

2. Number partitioning optimization and the trap model

From an optimization point of view, the unconstrained NPP is the following: given a set of real numbers $a_1, a_2, \ldots, a_N$, each one belonging to [0, 1], find a partition composed of two subsets such that the difference between the sum of numbers over the two subsets is as small as possible. It can be written as an infinite range Ising spin glass with Mattis-like antiferromagnetic couplings $J_{ij} = -a_i a_j$,

$$H_{\text{Mattis}} = E_m^2 = \sum_{i,j=1}^{N} s_i a_i a_j s_j \tag{1}$$

or, alternatively

$$E_m = \left| \sum_{i=1}^{N} a_i s_i \right| . \tag{2}$$

The ground state (for typical a_j) of (2) scales like $\langle E_{m_o} \rangle \propto \sqrt{N} 2^{-N}$ [7]. This means that in the form (1) of the Hamiltonian, the system is such that the interesting behaviour occurs at exponentially small temperature in terms of the size of the system. In order to avoid this problem, in this paper we shall use a modified Hamiltonian, whose ground state energy is extensive in the thermodynamic limit:

$$E = T_c \ln(E_m) = T_c \ln \left| \sum_{i=1}^{N} a_i s_i \right| . \tag{3}$$

T_c is an energy scale and the ground state energy becomes $\sim -T_c N \ln 2$.

2.1. Equilibrium analysis

Non-extensive optimization problems, for which the optimum does not scale linearly with the system size, are not easily cast in the formalism of statistical mechanics. For the NPP, Mertens [7] proposed a clever bypass: instead of working with a partition function defined on the basis of (1) or (2) and following the usual steps of computing the average free energy, he used statistical means to study directly the independence of energy levels. Thus, he argued that in the case of unconstrained NPP, for large values of N energies E_m are random variables distributed according to

$$P(E_m) = \frac{2}{\sqrt{2\pi\sigma^2 N}} \exp\left(-\frac{E_m^2}{2\sigma^2 N} \right) \Theta(E_m) \tag{4}$$

where $\Theta(E_m)$ is the step function and $\sigma^2 = \langle a^2 \rangle$, and that for $E_m < O(\sqrt{N})$ they are independent. This result was later shown rigorously for the lowest k energies [8], and studied in great detail in all regions in [9].

From this it follows, applying the transformation $E = T_c \ln |E_m|$, that energies $E < O(\ln N)$ are also independent random variables with a probability distribution given by

$$P(E) = K(N) \exp\left(\beta_c E - \frac{1}{2\sigma^2 N} \exp(2\beta_c E) \right) \tag{5}$$

with $K(N) = \frac{2\beta_c}{\sqrt{2\pi\sigma^2 N}}$. For large N, the density of levels is shown in figure 2.

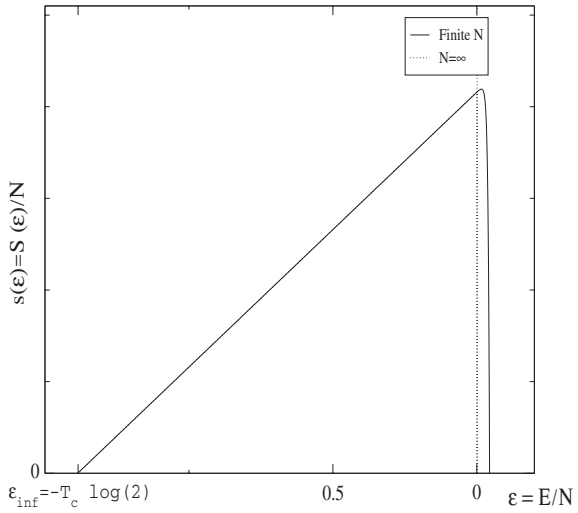

Figure 2. Entropy per spin $s = \frac{S}{N}$ versus energy per spin $\varepsilon = \frac{E}{N}$.

The thermodynamics of the NPP written in terms of the new energy E with assumptions above can be obtained following Derrida's microcanonical derivation for the random energy model [10]. One first notices that there are two energy regions:

- If $E > E_{\text{inf}} = -NT_{\text{c}} \ln 2$, the density of levels is much larger than 1.
- If $E < E_{\text{inf}} = -NT_{\text{c}} \ln 2$, the density of levels is much smaller than 1.

For $E < E_{\text{inf}}$ the entropy vanishes, and for $E \geqslant E_{\text{inf}}$, the entropy reads, as $N \to \infty$,

$$\frac{S(E)}{N} = \ln 2 + \frac{\beta_{\text{c}} E}{N} \Theta(-E). \tag{6}$$

Using the relation $\frac{\mathrm{d}S}{\mathrm{d}E} = \frac{1}{T}$, one finds that $\frac{E}{N} = 0$ when $T > T_{\text{c}}$, and that for $T < T_{\text{c}}$, the energy sticks at $E_{\text{inf}} = -T_{\text{c}} N \ln 2$. Finally, the free energy reads

$$\begin{cases} \frac{F}{N} = \frac{E_{\text{inf}}}{N} = -T_{\text{c}} \ln 2 & \text{if} \quad T < T_{\text{c}} \\ \frac{F}{N} = -T \ln 2 & \text{otherwise.} \end{cases}$$

This is a first-order transition [11], unlike the standard random energy model transition, which is second order. Let us stress here that above an energy $E_{\text{sup}} = O(\ln N)$ the density of states is again much smaller than 1. At this level, independence of energies is no longer expected [7]. In what follows, we shall be interested in transitions that involve low-energy states so that these levels are not relevant. We shall not study any statistical property of levels picked at random, this is done in [7, 8] and in all detail in [9]. We shall concentrate on the properties of energy levels *as encountered by a specific dynamics*, a related though clearly inequivalent question.

2.2. Dynamical analysis

The equilibrium calculation shows that the system maximizes its entropy at temperatures greater than T_{c}. In the low temperature phase $T \leqslant T_{\text{c}}$, a *metropolis* dynamics of the system explores deep states in its attempt to lower the energy down to $-N \ln 2N$. We shall argue that single spin-flip dynamics naturally leads to a trap model, and perform numerical tests

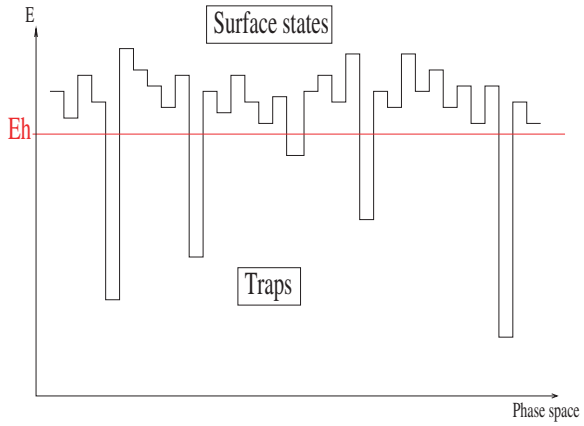

Figure 3. Phase-space structure defining traps and surface states.

to substantiate this claim. The metropolis dynamics is defined by transition rates verifying *detailed balance*:

$$P(\{\sigma_i\} \to \{\sigma_j\}) = \begin{cases} \exp(-\beta(E_j - E_i)) & \text{if} \quad E_j > E_i \\ 1 & \text{otherwise} \end{cases} \tag{7}$$

where $\{\sigma_i\}$ and $\{\sigma_j\}$ are configurations that differ by a single spin flip. Below T_c already an $N = 30$ spin system cannot be equilibrated in reasonable computer time.

2.2.1. Surface states and horizon. As mentioned above, one of the defining features of the trap model is a horizon level to which the system has to return each time it escapes a trap. Let us show that a single-flip dynamics naturally leads to this. When

$$E < E_h = T_c \ln(a_{\min}) \sim -T_c \ln N \tag{8}$$

with $a_{\min} \equiv \min(a_1, \ldots, a_N) = O(1/N)$, a single spin flip necessarily leads to a state whose energy is greater than E_h. In the present paper, we call a *trap* a state whose energy is lower than E_h and a *surface state*, a state whose energy is higher (see figure 3). It will turn out that for long times the system is dominated by long stays in deep traps, separated by rapid excursions close to the horizon level.

A quick first check can be obtained by looking at the energy evolution. Figure 4 shows a run for an $N = 10\,000$ spins system at temperature $T = 0.75T_c$. It appears that the expected scaling invariance of traps is well verified. Also a necessary condition, the system looks statistically invariant with respect to time reversal (cf figures 4(a) and (d)). Let us again stress this point that the trap model is time reversible in an interval between any two exits: *once a trap is left the system is as unoptimized as it was at the start*, when the system is in a deep trap, it has no other choice but to entirely reorganize itself to get to a new deep trap. An amusing exercise is to reconcile reversibility with the systematic trend of energy decrease we see in figure 5.

The existence of the horizon level is a direct consequence of the one-flip dynamics we have chosen, which forces deep traps to be many steps away from one another. Indeed, the very same system that allowed us to flip $O(N)$ spins each step has an entirely different dynamics: the jumps tend to go to deeper levels at each step, and figures like 4(a) and (d) would look completely different.

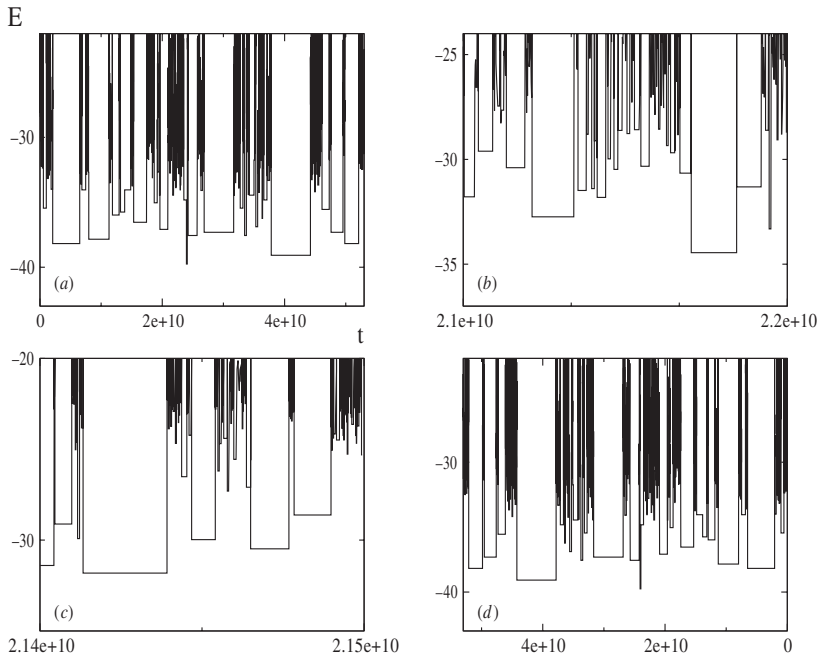

Figure 4. Energy versus time for a single run. (*a*) Whole run; (*b*) time magnification by 10; (*c*) time magnification by 100; (*d*) inverse time.

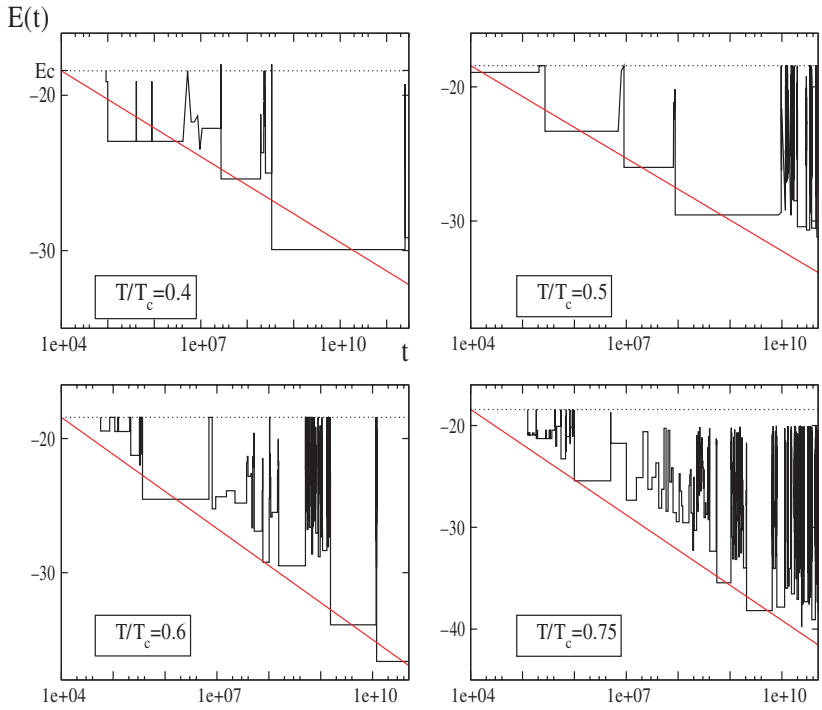

Figure 5. Time dependence of energy $E(t)$ for single runs at different temperatures, $N = 10\,000$. Straight lines are obtained from (20).

2.2.2. Time and energy distributions. Let us first examine the transition rates in order to determine the trapping time distribution. In a first stage, we assume the system to be in a trap, that is $E < E_h$: the only way to escape is to reach a higher energy state. If we note $x = \sum_{i=1}^{N} a_i s_i$, the probability to escape from x by a single spin flip reads

$$P_{\rm esc}(E(x)) = \frac{1}{N}\sum_i \exp\left(-\frac{T_{\rm c}}{T}(\ln|x - 2a_i s_i| - \ln|x|)\right). \tag{9}$$

If $|x|$ is much smaller than $a_{\min}$ ($\Longleftrightarrow E \ll E_h$):

$$P_{\rm esc}(E) = \frac{A_N}{N}\,{\rm e}^{\beta E}. \tag{10}$$

Here $A_N \equiv \sum_i^N a_i^{-\frac{T_{\rm c}}{T}}$ is the sum of N random variables with distributions with power-law tails $p\big(X = a_i^{-\frac{T_{\rm c}}{T}}\big) \sim X^{-(1+\frac{T}{T_{\rm c}})}$ for $T < T_{\rm c}$. This implies that for large N it becomes distributed according to a Levy law, and hence [12] $\bar{A}_N \sim N^{\frac{T_{\rm c}}{T}}$ and $\bar{A}_N^{-1} \sim N^{-\frac{T_{\rm c}}{T}}$. We thus have

$$\tau(E) = \tau_0\,{\rm e}^{-\beta E} \tag{11}$$

$$\tau_0 \propto N\,{\rm e}^{\beta E_h} \tag{12}$$

where τ_0 sets the timescale. Using the relation

$$\psi(\tau) = P(E)\left|\frac{\partial E}{\partial \tau}\right| \tag{13}$$

where $P(E)$ satisfies (5), we recover a Levy trapping time distribution:

$$\psi(\tau) \propto \frac{\tau_0^{\frac{T}{T_{\rm c}}}}{\tau^{1+\frac{T}{T_{\rm c}}}}. \tag{14}$$

If instead of assuming that one starts from a surface state, one computes the distributions of energies (or, equivalently, trapping times τ) as encountered at given time t_w, one obtains distributions modified by the observation time. If we consider the probability of being at t_w in a trap near the horizon, it is reasonable to assume that these are populated with a probability proportional to the Gibbs weight (with, of course, a cutoff at lower energies). We hence have

$$P_E(E, t_w) \propto \exp(-(\beta - \beta_{\rm c})E) \tag{15}$$

which implies, using the change of variables $P_\tau(\tau, t_w) = P_E(E, t_w)\left|\frac{{\rm d}E}{{\rm d}\tau}\right|$,

$$P_\tau(\tau, t_w) \propto \frac{\tau_0^{T/T_{\rm c}-1}}{\tau^{T/T_{\rm c}}} \qquad \tau \ll t_w. \tag{16}$$

In the opposite limit of deep energies, one may assume that two very deep states are visited with the same probability. One can prove this for the trap model, but here it remains a conjecture, just like all independence properties. In any event, this would lead to

$$P_E(E, t_w) \propto \mathcal{N}(t_w)\,{\rm e}^{\beta_{\rm c} E} \tag{17}$$

$$P_\tau(\tau, t_w) \propto \frac{\mathcal{N}(t_w)}{\tau^{1+T/T_{\rm c}}} \qquad \tau \gg t_w \tag{18}$$

demanding that $\int_{t_w}^{\infty} P_\tau(\tau, t_w)\,{\rm d}\tau$ stays of order 1, we have that $\mathcal{N} \sim t_w^{T/T_{\rm c}}$. More generally, considering that surface states have also Gibbsian weights, one can write a formula valid in all regimes [1, 3],

$$P_E(E, t_w) = \exp(-(\beta - \beta_{\rm c})E)\,r\left(\frac{\tau_0\,{\rm e}^{-\beta E}}{t_w}\right) \tag{19}$$

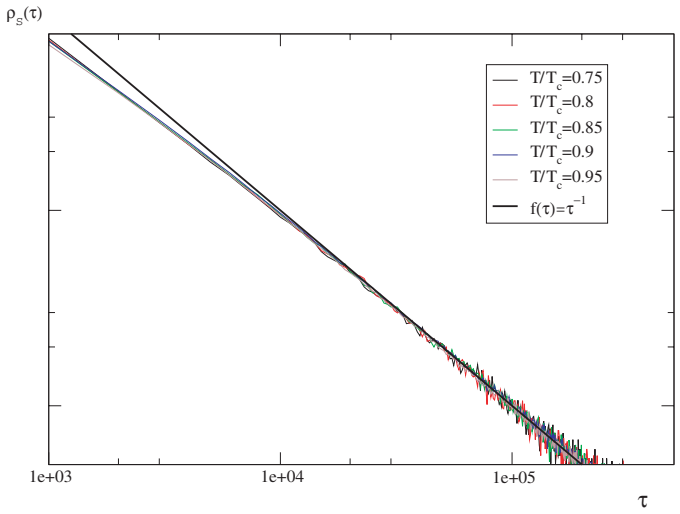

Figure 6. Rescaled trapping time distribution at $t_w = 10^4$ for $N = 1000$ spins.

where $r(u) = 1$ when $u \ll 1$ and $r(u) \sim u^{-1}$ when $u \gg 1$. In particular, we have on average

$$\langle E(t) \rangle \sim -T_c \ln \left(\frac{t}{\tau_0} \right)^{\frac{T}{T_c}} \tag{20}$$

where τ_0 is given by (12). In figure 5, we plotted different runs at different temperatures for a system of 10 000 spins in order to show the validity of (20). For different N similar curves are obtained.

From our NPP simulations, we computed the distribution (18) at different waiting times t_w. Figure 6 shows the rescaled probability $P^*_\tau(\tau, t_w) = (P_\tau(\tau, t_w))^{\frac{1}{1+\frac{T}{T_c}}}$ for a system of $N = 1000$ spins at $t_w = 10^4$ Monte Carlo steps, for different temperatures from $T = 0.7T_c$ to $T = 0.95T_c$. The curves are again in excellent agreement with what would have been obtained for the trap model.

In figure 7 we plot the energy of 50 spins obtained at $t_w = 2 \times 10^4$ for different runs, at three different temperatures. The straight lines correspond to the flat measure for the low-energy tails, and the Gibbs distribution for the high-energy tails. The agreement with the trap model behaviour is excellent.

2.2.3. Correlation between deep traps. The correlation between states of given energy in the NPP has been the object of detailed study following the proposal of Mertens [7–9]. Although these studies are no doubt relevant to the present work, one cannot transfer the results directly: while in a static study we consider the correlation of *any* two states below a certain energy, we are here forced to consider the correlation between states as visited by the dynamics. For example, if we demand that two states be visited subsequently, given one state, we are considering a very specific subset for the next. In other words, dynamics may impose correlations on statistically independent energy levels, and if independence emerges, it will be the result of a property of the dynamics.

As we shall see, another related question is the following: in the NPP, the natural way to define the correlation between configurations, based on the spins s_i is

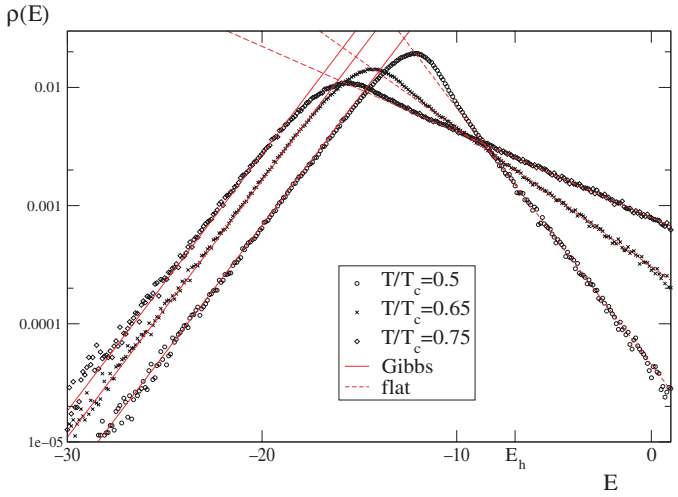

Figure 7. Energy distribution for different runs of a 50 spins system at $t_w = 2 \times 10^4$.

$$C_{\text{Single}}(t_w, t_w + t) = \frac{1}{N} \sum_{i=1}^{N} s_i(t_w) s_i(t_w + t). \tag{21}$$

On the other hand, the usual correlation studied in the trap model is defined as

$$C^B_{\text{Single}}(t_w, t_w + t) = \begin{cases} 1 & \text{if} \quad s_i(t + t_w) = s_i(t_w) \quad \forall\, i \\ 0 & \text{otherwise} \end{cases} \tag{22}$$

We shall later consider also the average correlation functions $C(t_w, t_w{+}t) = \langle C_{\text{Single}}(t_w, t_w{+}t)\rangle$ and $C^B(t_w, t_w + t) = \left\langle C^B_{\text{Single}}(t_w, t_w + t)\right\rangle$ ($\langle\cdot\rangle$ denotes the average over the noise history). Due to the characteristics of the trap model, it turns out that in the low-temperature phase, and for large waiting times, the two correlations coincide. The reason is interesting in itself: at long times, the system spends most of the time in deep traps. Now even though on average the passage between two deep traps takes for larger t_w less and less proportion of the time, it still involves many spin flips. Figure 8 shows this for different single runs with $N = 1000$ at $T = 0.75T_c$. As $t_w \to \infty$, we see that the correlation $C_{\text{Single}}(t_w, t_w + t)$ becomes essentially a single jump process: this is because the route separating two traps of typical life t_w becomes long.

Another way of confirming the increasing decorrelation during each passage over the horizon is to compute the first $\mathbf{s}_{\text{first}}$ and second $\mathbf{s}_{\text{second}}$ configurations to be visited under the condition that their energies are smaller than a given energy E^*. Their overlap $q = \mathbf{s}_{\text{first}} \cdot \mathbf{s}_{\text{second}}/N$ is the smaller, the lower the E^* considered.

We have also computed the averaged autocorrelation and the response function for a single sample:

$$C(t_w, t_w + t) = \frac{1}{N} \sum_{i=1}^{N} \langle s_i(t_w) s_i(t_w + t)\rangle \tag{23}$$

$$R(t_w, t_w + t) \equiv \sum_{i=1}^{N} \frac{\partial \langle s_i(t)\rangle}{\partial h_i(t_w)} = \int_{t_w}^{t_w+t} \mathrm{d}t' \, \frac{\delta m(t)}{\delta h(t')}. \tag{24}$$

The response is numerically obtained by computing $m(t) = \frac{1}{N}\sum_{i=1}^{N} \xi_i s_i(t)$ where $\{\xi_i\}$ is a set of independent random variables that can take the values ± 1. h is an external field coupled to

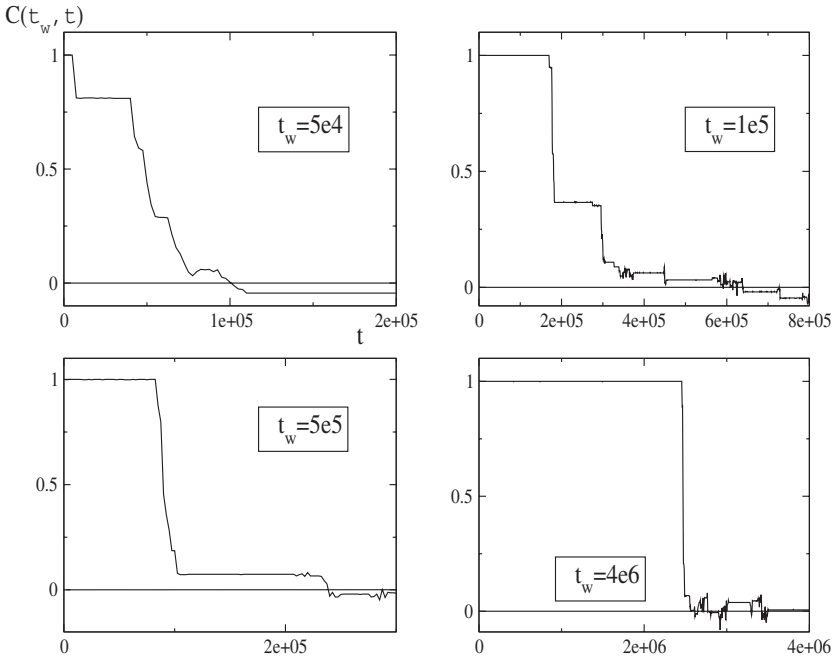

Figure 8. Single run correlation functions $\frac{1}{N}\sum s_i(t+t_w)s_i(t_w)$ for $N = 1000$; $T = 0.75T_c$. At longer times the behaviour approaches that of $C^B(t+t_w, t_w)$.

the spins via ξ_i. The interaction term involved in metropolis rates reads

$$E_h = E + V_h \qquad V_h = -h\sum_{i=1}^{N}\xi_i s_i. \tag{25}$$

At high temperature ($T > T_c$), the functions (23) and (24) become time translational invariant: there is no aging and the fluctuation–dissipation theorem holds (see figure 10).

At lower temperature, ($T < T_c$), the system is aging. We computed the autocorrelation (23) for an $N = 1000$ spins system at temperature $T = 0.75T_c$ and $N = 10\,000$ spins at $T = 0.9T_c$ for different waiting times t_w as a function of $\frac{t}{t_w}$. The results are given in figure 9. Firstly, we see that the longer we wait the better the scaling becomes. We also see that the long-time behaviour is well fitted by the analytical results of Bouchaud *et al* [3, 18],

$$C(t_w+t, t_w) \simeq \frac{\sin\left(\pi\frac{T}{T_c}\right)}{\pi}\int_{\frac{t}{t_w+t}}^{1} \mathrm{d}u(1-u)^{\frac{T}{T_c}-1}u^{-\frac{T}{T_c}} \tag{26}$$

but there is a long pre-asymptotic subaging regime. The inset of figure 9 shows that the higher the temperature, the longer the pre-asymptotic regime becomes.

In this section, we have shown evidence that in the limit $t_w \to \infty$, the present model becomes strictly the trap model: short-time discrepancies are due to the transition states in the frontier between surface states and traps. Note, however, that near the critical temperature, critical corrections to the asymptotical scaling $h\left(\frac{t}{t_w}\right)$ are also expected in the original trap model [13].

2.2.4. Out of equilibrium fluctuation–dissipation relations. One of the assumptions characterizing the trap model is the exponential distribution of energies. Given its close

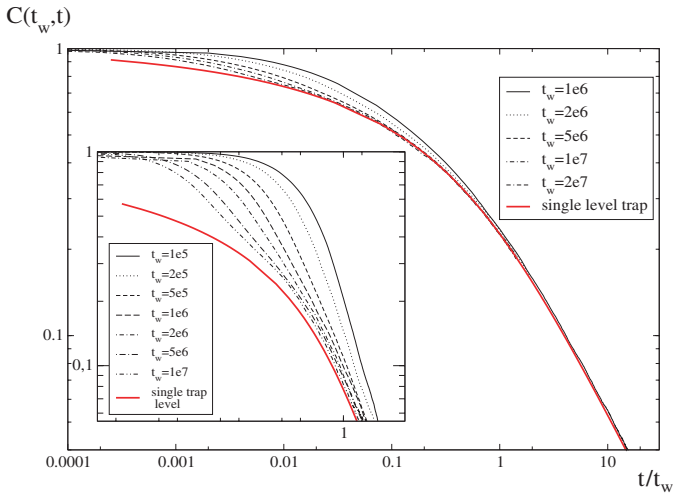

Figure 9. Autocorrelation function, $N = 1000$, $T = 0.75T_c$. Inset: $N = 10\,000$, $T = 0.9T_c$.

ties to the mean-field picture, and more importantly, to the 'entropy crisis' scenario of glasses, this is a feature one is reluctant to give up. In contrast, when it comes to specifying how the transition times are affected by a perturbation (such as a magnetic field), or equivalently, how a field affects the horizon level, there is considerable freedom. Indeed, given two states of energies E and E' with magnetizations M and M', respectively, the transition probabilities can be chosen as

$$P_{\rm esc}(\{M, E\} \to \{M', E'\}) = \exp(-\beta h[-(1-\zeta)M' + \zeta M])P_0(E \to E') \tag{27}$$

where $P_0(E \to E')$ is the rate without external field [3]. For any ζ, detailed balance is obeyed. One can thus show that the response becomes [3, 6]

$$R(t_w, t_w + t) = \beta\left(-\zeta\frac{\partial C(t_w,t)}{\partial t} + (1-\zeta)\frac{\partial C(t_w,t)}{\partial t_w}\right) \sim \beta\left[\zeta\frac{t_w}{t} + (1-\zeta)\right]\frac{\partial C(t_w,t)}{\partial t_w}. \tag{28}$$

If $\zeta = 0$ the rate is affected by the arrival configuration (at first sight a bizarre choice), and the fluctuation–dissipation formula holds. If $\zeta = 1$, when the rate depends on the departure configuration, there is a complicated fluctuation–dissipation relation that cannot be interpreted as resulting from an effective temperature (see [4, 5] for a detailed discussion).

The model studied here being 'microscopic', we have no freedom to choose how the magnetic field acts: the only reasonable choice is that the rates are given by the metropolis prescription with an additional energy term V_h (25). Figure 10 shows the fluctuation–dissipation characteristic at different temperatures above and below the critical temperature. Clearly, there is no FDT violation[3]. As we shall see, one expects this result to be general for microscopic models when the observables are smooth functions of the spins. To understand this lack of violation, first remark that it corresponds to the case $\zeta = 0$, as if the transition time did not depend on the original state. This is easy to understand: a smooth deformation of a golf course does not change the depths of the holes with respect to their edge; a single

[3] This result has already been found in the one-dimensional trap model [14], see [15] for an analytic proof of d-dimensional lattice trap models. Interestingly enough, such absence of violation of FDT is also present in some (very different) 'facilitated spin' models [16].

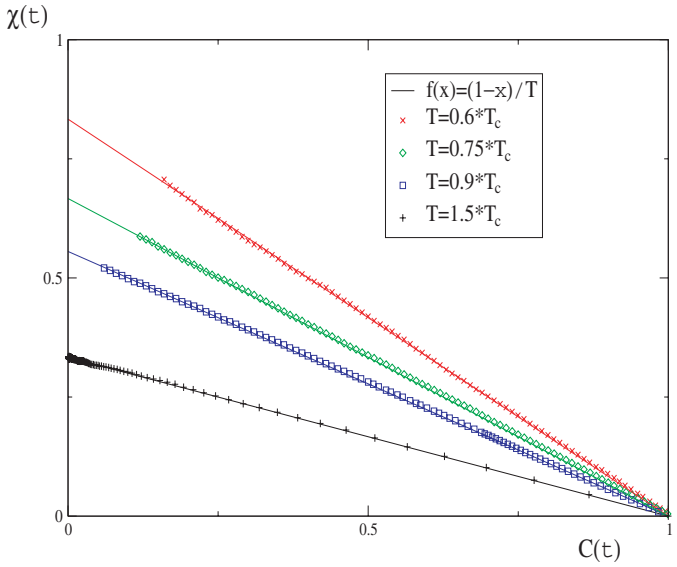

Figure 10. Fluctuation–dissipation relation for different temperatures above and below T_c. For $T = 1.5T_c, N = 10\,000, t_w = 1 \times 10^6$. For $T = 0.9T_c, N = 10\,000, t_w = 5 \times 10^6$. For $T = 0.6T_c, N = 1000, t_w = 5 \times 10^4$.

spin flip is enough to escape a hole but it does not change the magnetic energy! What is not obvious at this stage is how the magnetic field affects the choice of the *arrival* trap. To clarify this, we shall develop a rather different point of view based on the existence of superficial states that control the distribution of trap magnetizations.

We have the following picture for state distribution: there are surface states and there are traps that are reached from those states. Deep traps are separated by many surface (and short-lived) states, as we confirmed in the previous section. If the system is perturbed since the beginning by a small magnetic field, there is a small reshuffling in energy, but surface states remain on the surface.

Now, consider the time just before falling into a deep trap. The above consideration implies that the system is at the end of a tour consisting of many short-lived surface states. If we make the natural assumption that such states follow a Gibbs distribution even in the presence of a field, we conclude that the magnetization distribution just before falling is

$$P_{\text{before}}(M) = \frac{\int \mathrm{d}e\, P_{\text{sup}}(e, M)\, \mathrm{e}^{\beta h M}}{Z_h} = \frac{\mathrm{e}^{\beta h M} G(M)}{Z_h} \tag{29}$$

where $P_{\text{sup}}(e, M)$ is non-zero only when $e > E_h$. Z_h is the normalization factor. After falling into a trap, we know that the energy has changed dramatically. However, since the process of falling involves only one spin flip, the magnetization remains essentially unchanged (up to $O(1/N)$). Hence, the magnetization distribution inside a deep trap at a given time t is also of the form

$$P_t(M) = P_{\text{after}}(M) = \frac{\mathrm{e}^{\beta h M} G(M)}{Z_h} \tag{30}$$

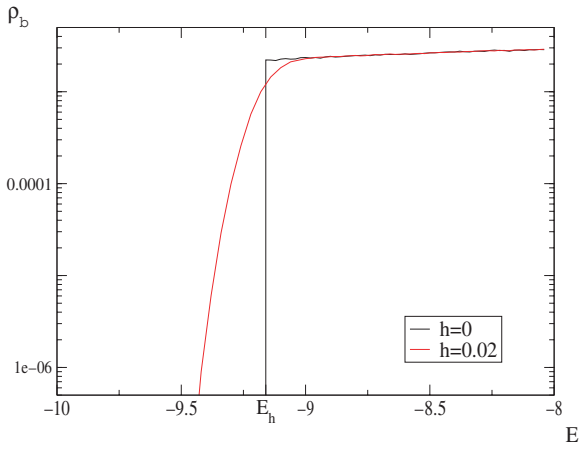

Figure 11. Energy density of states preceding traps. $N = 50$. $T = 0.75T_c$.

From this, the FDT result follows, since

$$\begin{aligned}\langle M\rangle &= \frac{\int \mathrm{d}M\, M\, \mathrm{e}^{\beta h M} G(M)}{Z_h}\\ \langle M^2\rangle - \langle M\rangle^2 &= \frac{\int \mathrm{d}M\, M^2\, \mathrm{e}^{\beta h M} G(M)}{Z_h} - \left(\frac{\int \mathrm{d}M\, M\, \mathrm{e}^{\beta h M} G(M)}{Z_h}\right)^2 \\ &= \beta^{-1}\frac{\partial\langle M\rangle}{\partial h}.\end{aligned} \tag{31}$$

We stress here that this argument will hold for *any* observable that, unlike the energy itself, is *smooth* in phase space (i.e., such that configurations that differ by a non-extensive number of spins have a negligible difference in the observable—in the opposite case, we describe them as *rugged*).

The fluctuation–dissipation relation in our model comes from a Gibbsian weight of states separating the traps. Numerical measurements confirm this scenario:

(1) We computed the energy of the last state visited by the system before falling into a trap. Figure 11 shows the results both with and without an external field. We can see that there is the announced zero-field horizon value for $E_h = T_c \ln(a_{\min})$ under which the system cannot reach a trap by a single flip. Comparison with figure 7 confirms that when an external field is added, the surface states essentially remain at the level of the zero-field surface, and are consequently still distributed following Gibbsian weights. Furthermore, the deviation with respect to E_h vanishes faster than exponentially.
(2) A direct consequence of our derivation is the density probability (30) for the magnetization. Figure 12 confirms the scaling $P(M) \propto \mathrm{e}^{\beta h M}$ for different values of T and small h.

From our analysis, the fluctuation–dissipation relation holds for smooth observables. The situation is different in the case of rugged observables. To verify this, we computed the fluctuation–dissipation relation in the case of an observable that resembles the magnetization but is restricted to be non-zero only when the energy configuration is less than $E_h = -T_c \ln(a_{\min})$:

$$\tilde{M}(\{s_i\}) = \begin{cases} \sum_{i=1}^{N} \xi_i s_i & \text{if} \quad E(\{s_i\}) < E_h \\ 0 & \text{otherwise.} \end{cases} \tag{32}$$

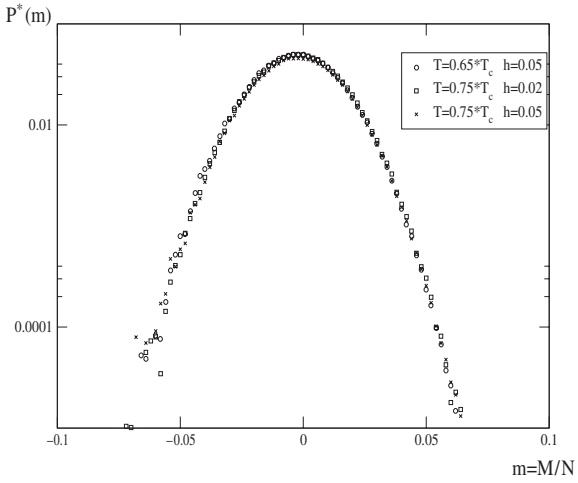

Figure 12. Rescaled distribution $P^*(M) = \mathrm{e}^{-\beta h M} P(M)$ for different values of h and T. Here, $m = \frac{M}{N}$ is the magnetization per spin. $N = 50$.

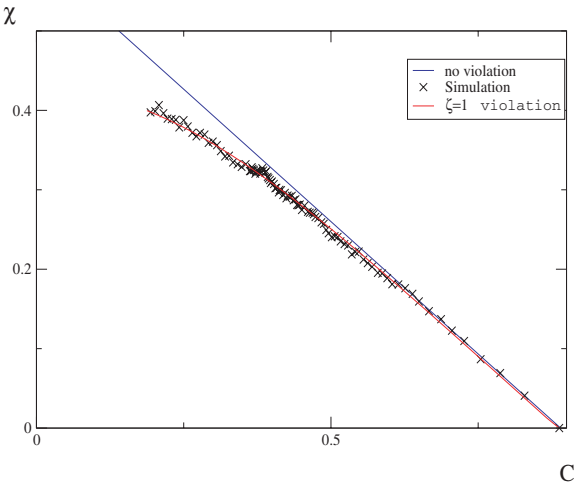

Figure 13. Fluctuation–dissipation relation for observable (32). $N = 50$. $T = 0.75T_c$. $t_w = 5 \times 10^4$. $h = 0.005$.

The fluctuation–dissipation plot is shown in figure 13. The violation follows the relation,

$$\tilde{R}(t_w, t) = -\beta \frac{\partial \tilde{C}(t_w, t)}{\partial t} \tag{33}$$

which corresponds to the case of $\zeta = 1$.

This result is not surprising. On one hand, since $\tilde{M}$ vanishes in the surface states it does not affect the dynamics between traps and is insensitive to the depth of the arrival trap. On the other hand, the probability to escape from a trap with $\tilde{M}$ is given by

$$P_{\mathrm{esc}}(\tilde{M}, E) \propto \exp(\beta(E - h\tilde{M})) \tag{34}$$

so that we have $\zeta = 1$.

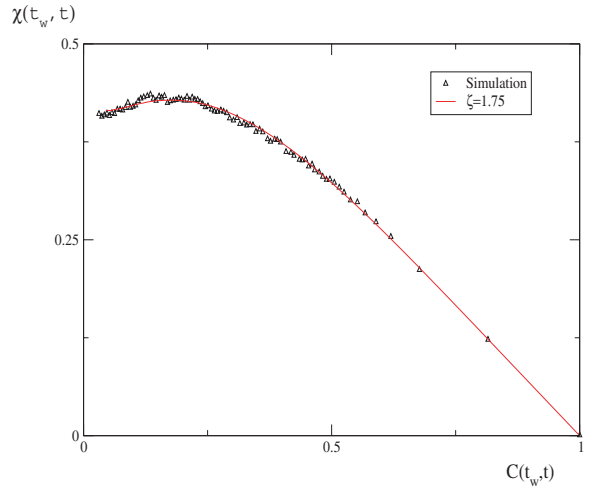

Figure 14. Fluctuation–dissipation relation in the case of parity observable.

We are now able to give a physical picture of the fluctuation–dissipation relations for all ζ. Consider an observable A that is the combination of two observables A_1 rugged (as (32)) and A_2 smooth,

$$A = \zeta A_1 + (1-\zeta)A_2 \tag{35}$$

and $\langle A_1^2(t_w)\rangle = \langle A_2^2(t_w)\rangle \to 1$. By definition A_1 verifies (33) and the equilibrium fluctuation–dissipation relation holds for A_2. Using linearity and the fact that for long times the autocorrelations of A_1 and A_2, become the same (a consequence of the dynamics of the trap model) one easily recovers the general case (28). Let us finally point out that the fluctuation–dissipation relation (28) is not restricted to values of ζ between 0 and 1. As an example, we report in figure 14 the fluctuation–dissipation relation for the parity:

$$P(\{s_i\}) = (-1)^{\frac{1}{2}|\sum_{i=1}^{N} s_i|}. \tag{36}$$

It yields fluctuation–dissipation plots with (28) $\zeta \sim 1.75$.

2.2.5. Nonexponential decay above T_c. Trap models exhibit interesting equilibrium dynamics in a range above T_c. Let us see how this comes about in our microscopic model. Consider first the canonical partition function associated with (3),

$$Z \sim \int_{E_{\rm inf}}^{0} \mathrm{d}E \exp(N\ln 2 - (\beta-\beta_c)E) \tag{37}$$

where $E_{\rm inf} = -NT_c \ln 2$. We make the change of variables,

$$n(E) = \exp(-\beta(E_h - E)) \tag{38}$$

where $n(E)$ represents the probability of escaping from a trap whose energy is E with the local dynamics (7). Then, Z can be rewritten as

$$Z \sim \exp(N\ln 2 - (\beta-\beta_c)E_h) \int_{\mathrm{e}^{-\frac{T_c}{T}N\ln 2}}^{\mathrm{e}^{-\beta E_h}} \mathrm{d}n\, n^{\frac{T}{T_c}-2}. \tag{39}$$

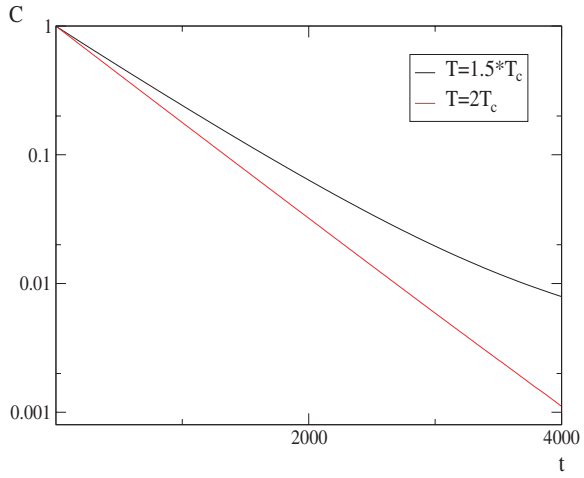

Figure 15. Correlation function above T_c; $N = 1000$.

Since E_h is not extensive and is independent of T, the free energy in the thermodynamic limit can be written as

$$\begin{aligned} F &= D - TN\ln 2 \\ D &\equiv -T\ln\left(\int_{2^{-\frac{T_c}{T}N}}^{1} \mathrm{d}n\, f(n)\right) \\ f(n) &= n^{\frac{T}{T_c}-2}. \end{aligned} \tag{40}$$

Three cases must be considered:

- $T > 2T_c$. In this case $\int_0^1 \mathrm{d}n\, f(n)$ is finite and D has a non-extensive contribution to the free energy.
- $T_c < T < 2T_c$. $\int_0^1 \mathrm{d}n\, f(n)$ is still finite and D has a non-extensive contribution, but $f(n)$ has a singularity at $n = 0$.
- $T < T_c$. This time $\int_\varepsilon^1 \mathrm{d}n\, f(n)$ diverges when $\varepsilon \to 0$, and hence D has an extensive contribution to the free energy.

We see that below $2T_c$ the equilibrium measure abnormally populates the dynamical states with low probability of escape $n(E) \sim 0$. This is the origin of time heterogeneities in dynamics and it naturally coincides with the divergence of trapping times' variance (14). As T is lowered, the effect of low n states in the dynamics becomes more and more pronounced [17–20], and the equilibration time finally diverges at T_c, when the states with low $n(E)$ become dominant. In figure 15 we compare the correlation function at $T = \frac{3}{2}T_c$ and at $T = 2T_c$. Although there is no aging and the system equilibrates, the correlation function has a long tail in the former, that is absent in the latter case.

2.2.6. Other trap distributions. The NPP can also be used as a microscopic basis for modified trap models. One may consider the definitions for the energy,

$$E^{\hat{\zeta}} = \left|\sum_i a_i s_i\right|^{-(1+\hat{\zeta})} \tag{41}$$

for $\hat{\zeta} > 0$, leading to non-extensive cost functions. Metropolis dynamics with this energy

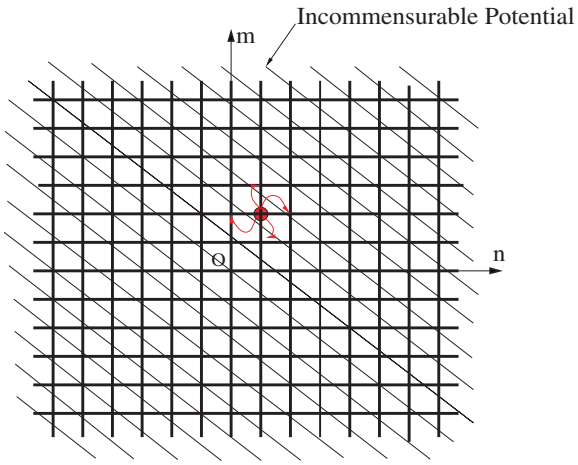

Figure 16. Two-dimensional diffusion with irrational steps. The diagonal lines represent the integer values of $n\sqrt{2}+m\sqrt{3}=$ even, where the energy is $-\infty$.

still goes in the right direction, but the dynamics is *not* trap model like. In fact, repeating the arguments above one finds trapping times distributed according to $P(\tau) \propto \tau^{-1}[\ln(\tau/\tau_0)]^{(1+\hat{\xi})}$. This case has also been discussed by Bouchaud [1]: at any temperature, one observes traps that become systematically longer in time.

3. Diophantine approximations

Number theory is a gold mine for glassy models without quenched randomness. This is because a program failing to find the good solution is trapped by the usually enormous number of near misses which behave as quasi-random numbers. Consider the problem of Diophantine approximations: we are asked, for example, to find integers n and m so that $n\sqrt{2}+m\sqrt{3}$ is as close as possible to an even integer. We can express this by saying that we want to minimize an energy

$$E = \ln\left\{F(n\sqrt{2}+m\sqrt{3}+2)\right\} \tag{42}$$

where $F(x)$ is the separation between x and its nearest even integer. One can view this optimization problem as a diffusion of a particle in a bidimensional lattice (n, m) with a periodic potential (42) incommensurable with the lattice spacing (figure 16), so that the places with $E=-\infty$ are always missed.

Let us give an alternative representation. Figure 17 shows the same problem, where we have now plotted one period of the potential, and assumed periodic boundary conditions.

In this representation, *each move is a large step*, because it goes around the boundary. What this second representation suggests is that a succession of many moves amounts to generating a (pseudo)random number in the interval $(-1, 1)$: we can thus expect the equilibrium measure to be flat and $E=\ln|x|$. The energy density of states of energy E would then be exponential, since

$$P(E) = \left|\frac{\mathrm{d}x}{\mathrm{d}E}\right| \sim \mathrm{e}^{E}. \tag{43}$$

Now, given a point (n, m) that yields a good approximation to an even integer, moving to nearby points like $(n+1, m)$ or $(n, m+1)$ will completely spoil the approximation, since it

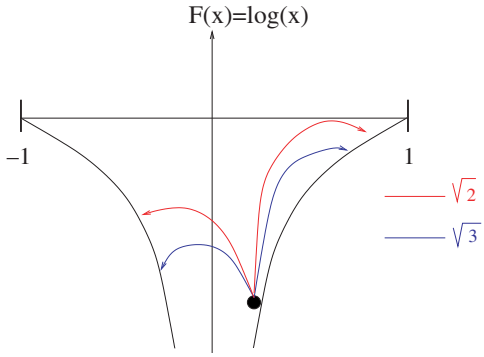

Figure 17. One-dimensional diffusion with irrational steps.

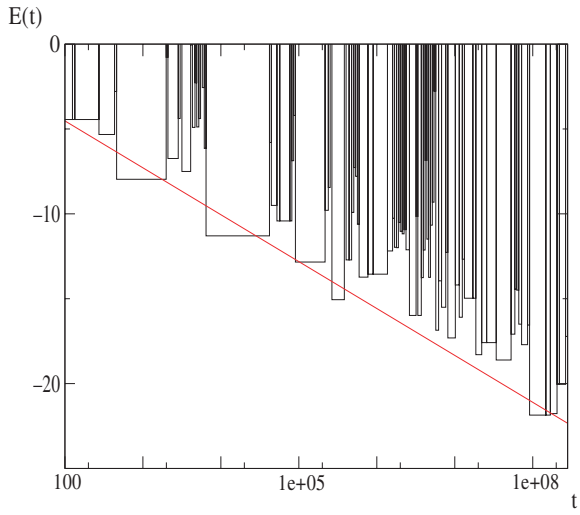

Figure 18. Approximating rationals as $p\sqrt{2}+q\sqrt{3}+r\sqrt{5}$, with p, q, r integers (see text).

implies jumps of $\sqrt{2}-1$ or $\sqrt{3}-1$. *This is a horizon as in the previous section: it is necessary to reemerge in order to find a deeper place*[4].

We can now make the assumption that at large, the diffusion process as viewed in figure 16 is a diffusion in a lattice with trapping times distributed according to a Lévy law. From what we know from such problems, returns are relatively frequent in two dimensions, somewhat changing the behaviour [22]. In order to make the comparison simpler, we have thus simulated a three-dimensional problem $E = \ln F\left(p\sqrt{2}+q\sqrt{3}+r\sqrt{5}+\frac{1}{2}\right)$. Figure 18 shows the behaviour of energy which looks just like in a trap model, the Levy flight leading to a subdiffusion process [22]. We have performed most of the tests as in the previous section, but the results being numerically indistinguishable, we do not present them here.

In order to stress the relevance of the horizon in the dynamics, consider the potential $\ln|x|$ with $x \in (-1, 1)$, with metropolis dynamics but with the configurations drawn each time at random in the interval $(-1, 1)$. One can easily check that the dynamics is *entirely different* from the trap model. The best way to convince oneself of this is to consider the limit $T = 0$:

[4] The situation is strongly reminiscent of the trapping in subrecoil laser cooling, see [21].

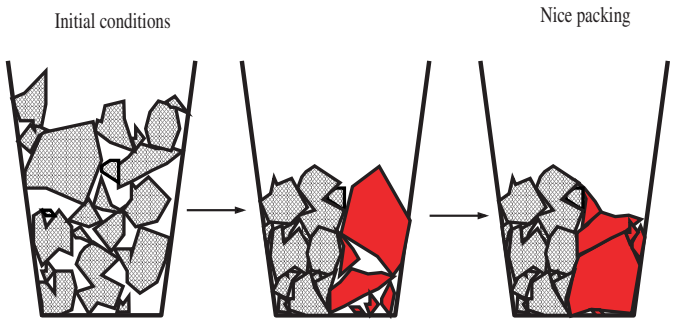

Figure 19. Direct compaction (left) at the first stages, global rearrangements as in the trap behaviour at late stages (right).

unlike the trap model, the system manages to decrease its energy monotonically without any activation, it suffices to wait long enough that the new configuration proposed has a sufficiently low new energy. On the one hand, we have a Bouchaud dynamics for the irrational jumps and on the other hand, we have a diffusion that resembles more the Barrat–Mezard model (where there is only descent) [23] if all steps are allowed. In the case of very small irrational steps, we can expect a crossover between these two regimes [24].

4. Discussion

4.1. Trap model behaviour

In this paper we have given two instances in which trap model like behaviour arises at long times, and we have used them to draw conclusions on what are the features required from a microscopic model for this to happen. A first obvious condition is the existence of states with a large distribution of trapping times. This, however, is not enough. As mentioned several times in this paper, the trap model is such that once the system emerges from a trap to a 'horizon' level, it is completely reinitialized. Furthermore, it is reversible in the sense that given a time interval delimited by two escapes, the history within it is equally probable as its time-reversed one. Irreversibility only arises because the fraction of time the system spends near the horizon becomes progressively smaller, although it never vanishes.

The question one may ask is under what circumstances can one have a horizon level with such a property. Considering the NPP as the problem of minimizing the height of a box needed to pack two piles of coins of random thicknesses, we have seen that the horizon level arises when the system has been optimized up to the thickness of the thinnest coin: after that, any swap of coins will necessarily bring the system back to the horizon, and improvements only result after global rearrangements. One has then a crossover between irreversible early dynamics, where single swaps may be advantageous, to a trap/reinitialization dynamics at longer times. One may conjecture that this might be quite general for packing problems.

Glass systems and granular matter have no doubt a first regime of irreversible compaction, during which a trap (whenever we are able to define one) is most probably followed by a deeper trap, and this is also the case of the dynamics of schematic models. Thus, one can envision true trap model behaviour arising at extremely long times, when each improvement requires complete reshuffling: this will surely happen at the level of optimization of a few grains (figure 19), in agreement with the analysis for the random energy model [2]. Another, perhaps more relevant situation could arise at shorter times, but considering the trap behaviour of subsystems separately.

4.2. Fluctuation–dissipation relation

One of the main conclusions of the analytic solutions of glassy dynamics [6] is the central role played by the fluctuation–dissipation relations. It has hence become standard practice to study numerical and experimental systems from this point of view, and quite naturally one is led to look at this question in the trap model. As we have mentioned above, the model as it stands allows for great freedom in this respect: since we are free to specify how the fields modify the barriers, the response to a field can strongly depend on this prescription. One of the main points of this paper is that for observables that are smooth functions of the microscopic variables, the fluctuation–dissipation relation holds in the aging phase just as in equilibrium. Although we have shown this for the two specific models, the argument seems robust enough (so that it rationalizes *a posteriori* the results of [14, 15]): the energy being rugged, escaping a deep trap involves a few steps, a distance along which a smooth variable does not vary. Only long trajectories feel spatially smooth perturbations, and these happen near the horizon level which can be assumed to be in local equilibrium. Let us note here that smooth variables cannot be correlated with the energy, which is itself rugged, so they are 'neutral' in the sense of Sollich [4]: they are not 'what is being compactified'.

Once again we find confirmation that trap model behaviour can only arise at very long times: for example, in mean-field models even within the activated regime one has initially a violation of the equilibrium fluctuation–dissipation relation [25], and the emergence of an effective temperature. This means that if these models eventually cross over to trap model behaviour, this will be only after the effective temperature has thermalized with the bath temperature, and this is expected to happen when energies are barely (to $O(N)$) above the equilibrium energy. It would be interesting to understand this crossover better, as it may be relevant for finite-dimensional models.

4.3. Optimization and non-extensivity

The NPP is non-extensive if one defines the energy as the absolute value of the difference, in the sense that the ground state energy scales as an exponential of the size, or equivalently, that in a thermodynamic construction the interesting temperatures are exponentially close to zero. Working with temperatures that depend on the size is always awkward, so we have chosen a new energy as the logarithm of the old one. This immediately led to a well-defined thermodynamics and, via metropolis dynamics, to trap model behaviour.

Because the trap model is by construction forgetful of its history, its appearance in an optimization algorithm is a sign that things are as bad as possible. Indeed, our scaling forms for the dynamics immediately yield exponential times to reach the ground state—essentially what one would have obtained by blind enumeration. An interesting property one can check is that, not surprisingly *the best temperature from the point of view of optimization is the critical temperature*.

Acknowledgments

We wish to thank E Bertin and J-P Bouchaud for useful suggestions, and S Franz for discussing his unpublished results.

References

[1] Bouchaud J-P 1992 *J. Physique* I **2** 1705
[2] Ben Arous G, Bovier A and Gayard V 2002 *Phys. Rev. Lett.* **88** 087201
Ben Arous G, Bovier A and Gayard V 2003 *Commun. Math. Phys.* **236** 1–54

[3] Bouchaud J-P and Dean D S 1995 *J. Physique* I **5** 265
[4] Fielding S and Sollich P 2002 *Phys. Rev. Lett.* **88** 050603
Sollich P 2003 *J. Phys. A: Math. Gen.* **36** 10807
[5] Ritort F 2003 *J. Phys. A: Math. Gen.* **36** 10791
[6] Bouchaud J-P, Cugliandolo L F, Kurchan J and Mezard M 1997 *Spin Glasses and Random Fields* ed A P Young (Singapore: World Scientific) (*Preprint* cond-mat/9702070)
[7] Mertens S 2000 *Phys. Rev. Lett.* **84** 1347
Mertens S 2001 *Theor. Comput. Sci.* **265** 79
[8] Borgs C, Chayes J and Pittel B 2001 *Random Struct. Algorithms* **19** 247
[9] Bauke H, Franz S and Mertens S 2004 Number partitioning as random energy model *Preprint* cond-mat/0402010
[10] Derrida B 1980 *Phys. Rev. Lett.* **45** 79
[11] Bouchaud J-P and Mezard M 1997 *J. Phys. A: Math. Gen.* **30** 7997
[12] Bouchaud J-P and Georges A 1990 *Phys. Rep.* **195** 127
[13] Bertin E private communication
[14] Bertin E and Bouchaud J-P 2003 *Phys. Rev.* E **67** 065105(R)
[15] Monthus C 2003 *J. Phys. A: Math. Gen.* **36** 11605
[16] Buhot A and Garrahan J P 2002 *Phys. Rev. Lett.* **88** 225702
[17] Odagaki T 1995 *Phys. Rev. Lett.* **75** 3701
[18] Monthus C and Bouchaud J-P 1996 *J. Phys. A: Math. Gen.* **29** 3847
[19] Denny R A, Reichman D and Bouchaud J-P 2003 *Phys. Rev. Lett.* **90** 025503
[20] Berthier L and Garrahan J P 2003 *Phys. Rev.* E **68** 041201
[21] Bardou F, Bouchaud J P, Emile O, Aspect A and Cohen-Tannoudji C 1994 *Phys. Rev. Lett.* **72** 203
[22] Monthus C 2003 *Phys. Rev.* E **68** 036114
[23] Barrat A and Mezard M 1995 *J. Physique* I **5** 941
[24] Bertin E 2003 *J. Phys. A: Math. Gen.* **36** 10683
[25] Crisanti A and Ritort F 2000 *Europhys. Lett.* **51** 147